Hindawi
Adsorption Science & Technology
Volume 2022, Article ID 7244006, 9 pages
https://doi.org/10.1155/2022/7244006

Research Article

A Comprehensive Study on the Synthesis and Characterization of TiO_2 Nanoparticles Using *Aloe vera* Plant Extract and Their Photocatalytic Activity against MB Dye

S. Srujana,[1] **M. Anjamma**,[2] **Alimuddin**,[3] **Bharat Singh**,[4] **Ram C. Dhakar**,[5] **Shanthi Natarajan**,[6] **and Ramana Hechhu**[7]

[1]*Department of Biotechnology, School of Sciences, Jain University, J.C. Road, Bengaluru, 560027 Karnataka, India*
[2]*Department of Botany, Osmania University, Hyderabad, Telangana, India*
[3]*Physical Sciences Section, School of Sciences, Maulana Azad National Urdu University, Hyderabad, 500032 Telangana, India*
[4]*Department of Mechanical Engineering, GLA University, Mathura, India*
[5]*Department of Hospital Pharmacy, SRG Hospital and Medical College, Jhalawar, Rajasthan, India*
[6]*PG and Research Department of Botany, Pachaiyappa's College, Affiliated to University of Madras, Chennai, 600030 Tamil Nadu, India*
[7]*Department of Pharmaceutical Chemistry, School of Pharmacy, Wolaita Sodo University, Ethiopia*

Correspondence should be addressed to Ramana Hechhu; ramana@wsu.edu.et

Received 23 May 2022; Revised 22 June 2022; Accepted 28 June 2022; Published 28 July 2022

Academic Editor: R Lakshmipathy

This paper investigates the use of A. vera extract as a natural capping agent for TiO_2 nanoparticles as well as a reducing agent for TiO_2 nanoparticles. XRD, ultraviolet diffuse reflectance (UV-DRS), Fourier transform infrared spectroscopy (FT-IR), transmission electron microscopy (TEM), scanning electron microscopy (SEM), and energy-dispersive X-ray analysis (EDXA) were used to characterize the material. In their X-ray diffraction patterns, the titanium dioxide nanoparticles were found to have a high degree of crystallinity, indicating that they were synthesized. Infrared (FT-IR) spectra were used to determine the chemical composition of the plant extract. The DRS spectra in the UV-visible range reveal a high absorption peak at 356 nm, which indicates the existence of TiO_2 nanoparticles in the sample. Shape of nanoparticles was revealed by SEM and TEM morphological investigations, which revealed their irregular and somewhat spherical nature. Only titanium and oxygen compounds were found in the EDX spectrum, indicating that they were present. This demonstrates that the NPs that were produced are devoid of contaminants. Using the produced nanoparticles as catalyst, we presented a photocatalytic degradation method for the dye methylene blue in this paper. The findings showed that 94 percent of the damage occurred within 120 minutes of being exposed to UV radiation.

1. Introduction

Nanotechnology is a broad word that encompasses a wide range of applied scientific and technology domains that are defined by tiny size and huge surface areas, as well as the ability to exhibit exceptional and unique characteristics [1]. Recently, nanoparticles in a variety of forms and sizes have piqued the public's curiosity [2]. Nanoscience and nanotechnology have a variety of practical applications in the real world, including industry, environmental management, medicine, and food preservation [3, 4]. In order to avoid the use of potentially dangerous solvents during the synthesis of nanomaterials, pressures, temperatures, reaction atmospheric conditions, and a long refluxing duration were all meticulously monitored and regulated [4, 5]. Metal oxide nanoparticles are extensively employed in a variety of applications, including electrical, magnetic, and optoelectronic. Controlling the size of the NPs is an important parameter for a wide range of application scenarios. Microwave radiation, laser ablation, chemical reduction, sol-gel,

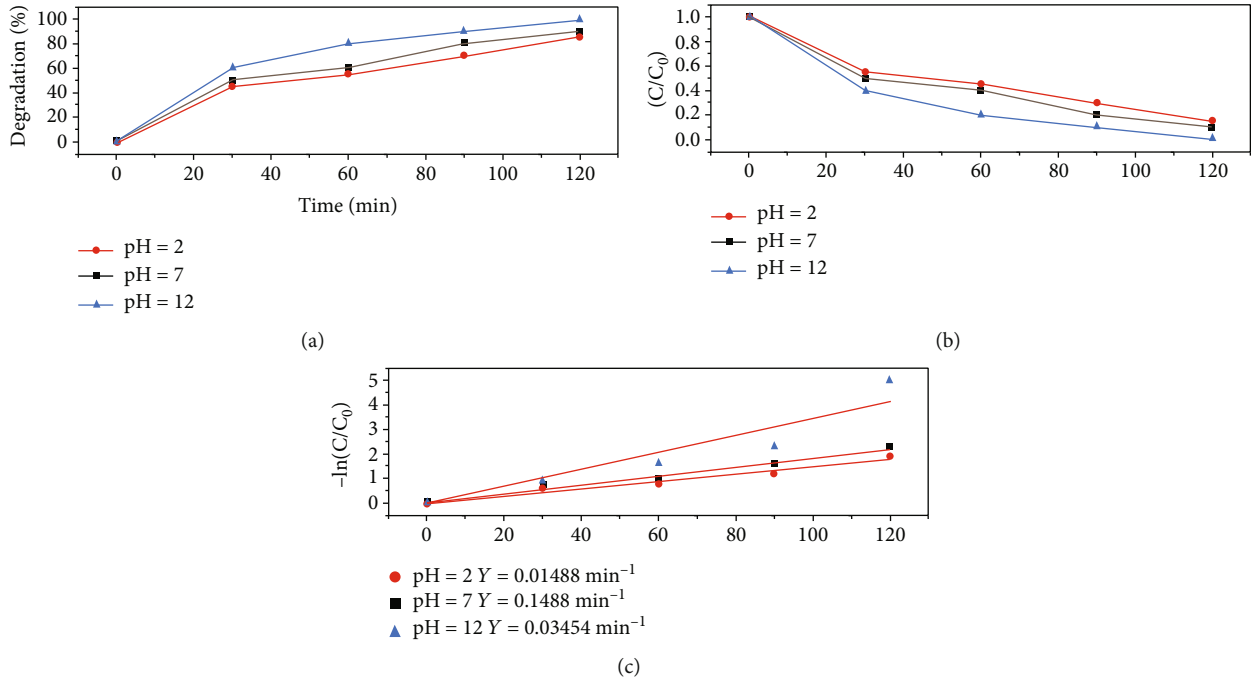

FIGURE 1: (a) Degradation efficacy of biosynthesized TiO_2 NPs with various pH, (b) C/C_0 absorption rate, and (c) photocatalytic degradation kinetics study of the biosynthesized TiO_2 NPs with various pH.

hydrothermal, and coprecipitation processes are all used to create metal and metal oxide nanoparticles [6–8]. Metal and metal oxide nanoparticles are also manufactured using a variety of chemical and physical methods. Chemical and physical processes have a number of significant limitations, including the use of dangerous chemicals, the need for rigorous environmental conditions such as proper temperature and pH, scalability challenges, and the production of poisonous by-products [9]. Biosynthetic processes have a number of advantages over chemical and physical techniques, and they have established themselves as an easy, safe, and practical alternative. As an alternative to this, biological approaches may effectively aid the synthesis process at all sizes and under all situations. It was necessary to create green technology in order to overcome the limits and downsides of traditional chemical synthesis. Green technology is a way of manufacturing nanoparticles (NPs) with high prospective attributes that have the ability to overcome application limitations in a variety of industries. In comparison to chemical synthesis, it is more cost-effective. As previously stated, it is devoid of potentially harmful chemicals and requires no costly machinery [10, 11]. It is also affordable [10, 11]. Because of the wide range of physical and chemical characteristics of titanium dioxide nanoparticles (NPs), the material has garnered a great deal of attention in the recent decade. TiO_2 is a photocatalytic material that is nontoxic and environmentally beneficial, and it has excellent optical characteristics, thermal solidification, and chemical stability. TiO_2 is used in a variety of products these days, including skincare treatments, culinary colourants, inks, and toothpaste. TiO_2 is also used to make diamonds. The chemicals are used in the production of tints, fabrics, papers, plastics, cosmetics, and meals [12, 13]. Hydrophobicity, nonwet ability, and a huge bandgap are only a few of the high-end characteristics of this material. Dye-sensitive solar panels, photocatalysis, self-cleaning, charge distributing devices, gas sensors, nanoelectronics, and photocatalysis are only a few of the industrial uses of nanoparticles [14–17]. Nanoparticles are also used in antimicrobial goods and textile products. Aloe vera is a kind of Aloe that is well-known for its medical capabilities. It is a succulent plant. "Alloeh" is an Arabic word that means "shining bitter stuff," and "vera" is a Latin word that means "truth." Aloe vera is a plant of the Liliaceae family, barbadensis Mill [18]. In addition to treating wounds and burns, aloe vera is used to treat lung cancer and digestive difficulties, boost HDL cholesterol while lowering bad cholesterol, reduce blood sugar in diabetics, battle AIDS and allergies, and strengthen the immune system [19–22]. A large number of nutrients and bioactive compounds are found in Aloe vera, which are responsible for the plant's medicinal benefits. Aloe vera contains hundreds of nutrients and bioactive chemicals. Vitamins, proteins, minerals, polysaccharides, flavonoids, phenolics, saponins, oxalic acid, and nucleic acids are only a few of the compounds that make up the human body's nutritional needs. Aloe vera has traditionally been used in traditional medical systems to treat burn injuries, rashes, cosmetic concerns, congestion, and fever [23, 24]. Flavonoids, steroids, phenylpropanoids, protein, phenolic compounds, carbohydrates, reducing sugar, starch, tannins, and glycosides are found in Aloe vera leaves [25]. Aloe vera leaves also include a variety of other substances. Titanium dioxide nanoparticles were minimised and manufactured using an Aloe leaf extract in aqueous solution (TiO_2 nanoparticles). The biosynthesis of

TiO_2 NPs was confirmed by UV-vis spectroscopy [26]. When combined with smaller MgO nanoparticles, as shown by HRTEM and FESEM study, Aloe barbadensis phytochemical extract may be employed for a variety of biological and biomedical applications [27, 28]. The antibacterial activity of zinc oxide (ZnO) derived from Aloe vera plant extract has been shown to be very effective against Escherichia coli [28]. Using an Aloe vera extract as a starting material, a green synthesis process was employed to create titanium dioxide nanoparticles in this study. The current project focused on two critical phases.

(1) The plant extract reduction was building the nanoparticles in below 100°C

(2) The synthesized nanoparticle catalytic activity was examined against MB dye

2. Experimental

2.1. Materials. To synthesize TiO_2 nanoparticles, titanium tetra isopropoxide was purchased (TTIP Sigma-Aldrich, AR grade, purity >99 percent). Fresh Aloe vera leaves were obtained and prepared to be used as a biotemplate. Methylene blue was maintained in a glass bottle in the refrigerator until needed for photocatalytic activity. TiO_2 nanopowder is shown in Figure 2.

The preparation flowchart of TiO_2 nanoparticles is included in Figure 3.

2.2. TiO_2 NP Green Synthesis. To synthesize titanium dioxide nanoparticles from the leaves of the Aloe vera plant, which is a naturally occurring source of titanium dioxide, the green synthesis approach was used. To get the final solution, a 0.1 M TTIP solution was mixed with 90 mL of aloe vera extract. After one hour of stirring, the colour changed from red to milk white, and the resultant precipitate was centrifuged at 1000 rpm for ten minutes three times, each time for a total of ten minutes. Centrifuged samples were cleaned with acetone and roasted at 100 degrees Celsius for eight hours after which they were cooled.

2.3. Characterization. The characteristics of nanoparticles were examined in this study. A 40 kV/15 mA radiation X-ray diffractometer equipment was used for studying the structural features of TiO_2 nanoparticles at temperatures ranging between 10° and 80°C. The Shimadzu 2700 UV-visible spectrophotometer was used to assess the absorption of titanium dioxide nanoparticles. SEM Carl ZEISS and energy-dispersive X-ray spectroscopy were used to characterize the green-generated TiO_2 nanoparticles before chemical analysis was performed using Perkin Elmer FT-IR spectroscopy 400-4000 cm^{-1} (EDXS). A TEM was used to investigate the nanoparticle's surface shape and texture (Titan).

2.4. Photocatalytic Activity. The photocatalytic effectiveness of TiO_2 nanoparticles was investigated using ultraviolet light and the dye MB as a model dye. The photocatalytic activity induced by ultraviolet light is one of the conformist approaches for the reduction of organic contaminants. The 10 mg catalyst was added to the 100 mL dye solution that

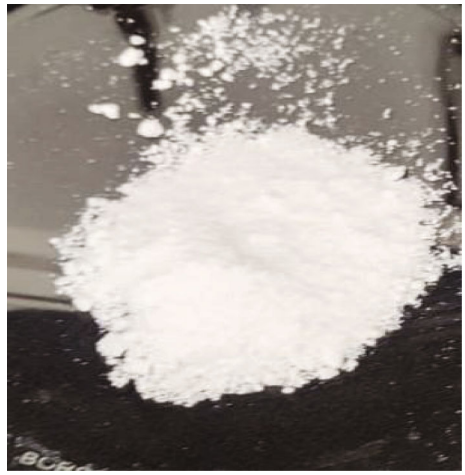

Figure 2: TiO_2 nanopowder.

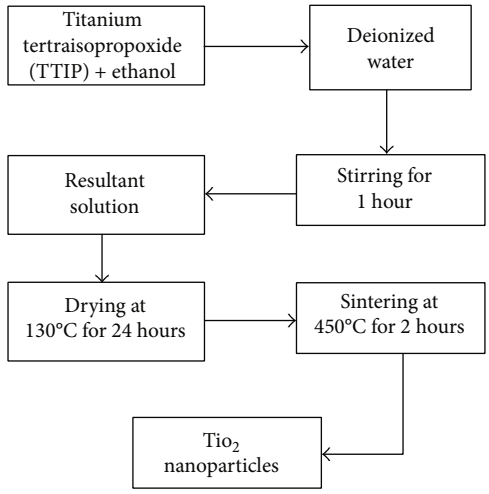

Figure 3: Preparation flowchart of TiO_2 nanoparticles.

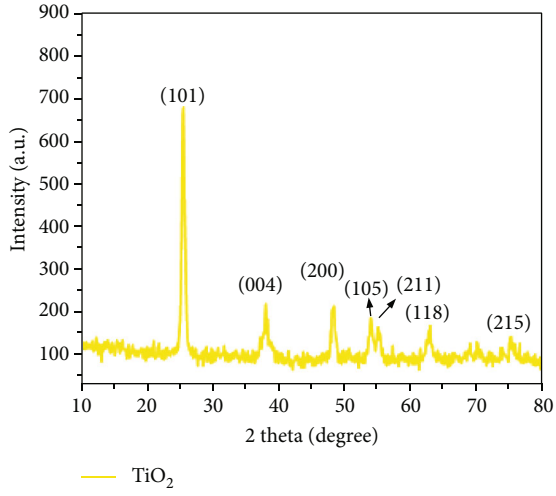

Figure 4: XRD crystalline nature of the synthesized TiO_2 nanoparticles.

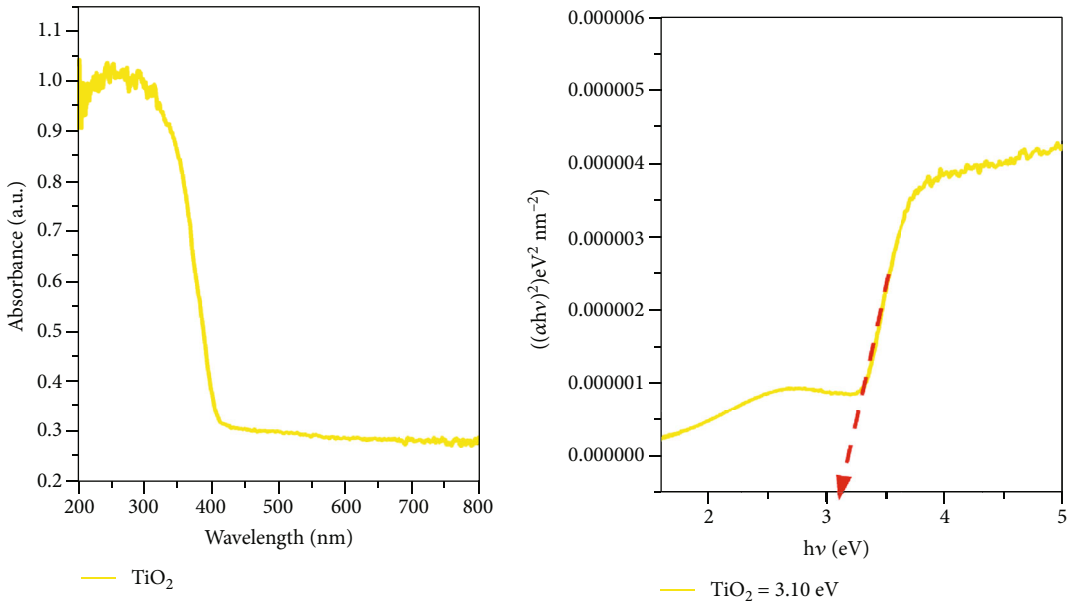

Figure 5: (a) Spectrum of UV-DRS absorption of biosynthesized TiO_2 NPs. (b) Synthesized NPs.

had been produced. The mixed solutions were maintained in a dark environment with no exposure to light. In the absence of light circumstances, it was much easier to obtain the optimum adsorption-desorption balance. The samples (3 mL) were collected out of the irradiated samples every 30 minutes to assess the degradation percentage of the loaded sample, which was irradiated with UV radiation.

The efficiency of dye degradation [29] was assessed as follows:

$$\text{Photocatalytic dye degradation}\,(\%) = \frac{C_0 - C_t}{C_0} * 100, \quad (1)$$

where C_0 is the absence of light of the dye at $time = 0$, C_t is the presence of light of the dye at time = 30 min, and t is the time.

3. Results and Discussion

3.1. XRD Analysis. The XRD pattern revealed the phase, purity, structural, and average crystallite size values of the TiO_2 nanoparticles, which are shown in Figure 4. X-ray diffraction showed peaks at 25.38 degrees, 37.97 degrees, 48.14 degrees, 54.40 degrees, 55.20 degrees, 62.73 degrees, and 75.4 degrees. These angles correspond to a Miller index value of (101), (004), (200), (105) (211), (118), and (215) correspondingly. JCPDS Card No. 78-2486, which is issued by the Joint Committee on Powder Diffraction Standards, was used in order to validate the findings that were gathered [30, 31]. The crystallinity of the NPs contributes to an increase in the photocatalytic activity, which can be seen in the form of a prominent peak. The equation developed by Debye and Scherrer was used in order to calculate the typical dimension of crystalline particles (Equation (2)).

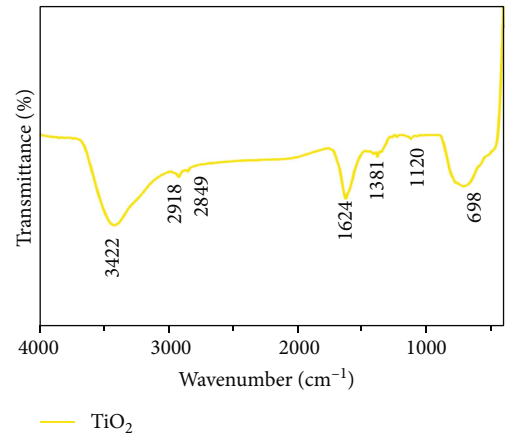

Figure 6: Biosynthesized TiO_2 nanoparticle FT-IR spectrum.

Debye-Scherrer's equation [32] is given by

$$D = \frac{0.89\lambda}{\beta \cos\theta}. \quad (2)$$

The (101) plane was selected to be used in the calculation of the crystalline size. The as-prepared TiO_2 NPs that were synthesized by utilising Aloe vera solution had a crystalline size of 27 nanometers. As a consequence of this, it is hypothesised that TiO_2 NPs have a larger surface area as well as dye molecules on their surface, which would lead to improved photocatalytic activity [33–36].

3.2. UV-DRS Analysis. The bandgap of green-route synthesized TiO_2 nanoparticles was investigated using a UV-visible spectrophotometer. The prepared TiO_2 nanoparticles display significant absorption in the UV range because of the

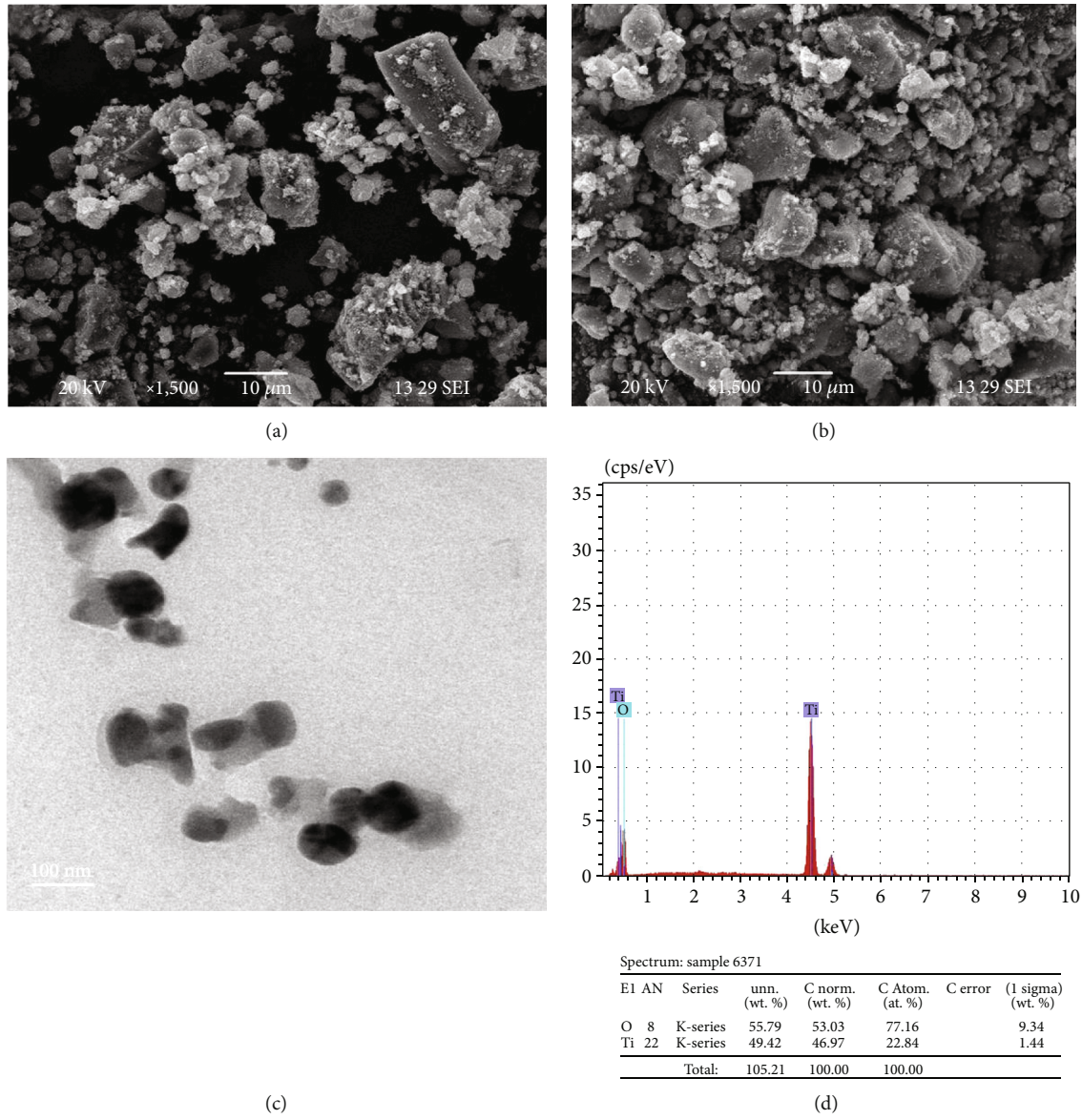

Figure 7: (a and b) TiO_2 NP SEM images, (c) TiO_2 NP TEM micrograph, and (d) TiO_2 NP EDX spectra.

broad forbidden bandgap transition and reduced absorption in the visible range due to surface imperfections in TiO_2 nanoparticles. The absorption of intrinsic bandgap in TiO_2 nanoparticles results in a prominent absorption peak at 356 nm [37]. Using Tauc's plot method, the optical bandgap of TiO_2 NPs was determined to be 3.1 eV (Figures 5(a) and 5(b)). The measured absorption edge of TiO_2 nanoparticles at 356 nm is markedly blue-shifted compared to tetragonal anatase TiO_2 nanoparticles' bulk bandgap wavelength (345 nm) [38].

The presence of a significant 356 nm spike in the wavelength range 200–600 nm supports the production of green TiO_2 nanoparticles. With Equation (3), you can figure out the energy gap of TiO_2 made with the green method [39].

$$E_g = h\frac{c}{\lambda}, \tag{3}$$

where E_g is the energy, h is Planck's constant, c is the speed of the light, and λ is the wavelength.

The UV-visible absorption spectra of TiO_2 demonstrate that it operates as a photocatalyst and responds significantly due to the production of reactive species in the exposed to UV light [40]. The particle's potential energy state is multiplied by the number of molecular orbitals in its vicinity for each molecular orbital. Thus, absorbance will occur at greater energies, resulting in shorter wavelengths, which will be absorbed.

3.3. FT-IR Analysis. Figure 6 shows TiO_2 NP spectra in the 400–4000 cm^{-1} range that were generated using a green chemical process. This curve [20, 21] shows O–Ti–O bonding at a peak of 698 cm^{-1} in a highly crystalline phase [20]. The bands for surface-adsorbed water and hydroxyl groups are each located at 1624 cm^{-1} and 3422 cm^{-1}. During the calcination of TiO_2 NPs, peaks in the C–H stretching band at

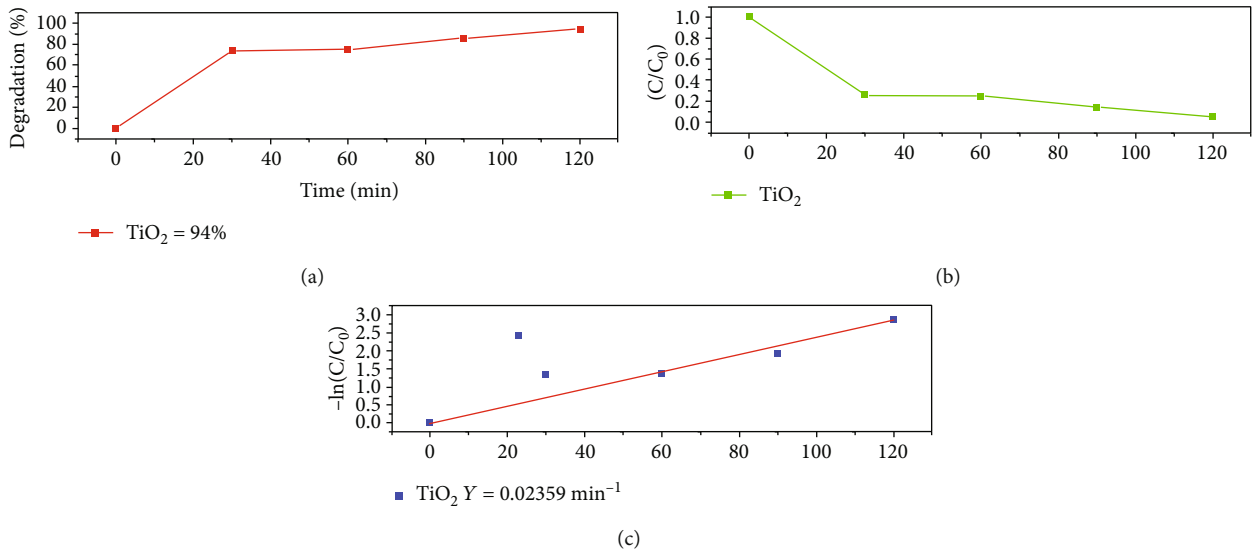

FIGURE 8: (a) Degradation efficacy of biosynthesized TiO_2 NPs for MB dye solution, (b) C/C_0 absorption rate, and (c) photocatalytic degradation kinetics study of the biosynthesized TiO_2 NPs.

2918 MHz and 2849 MHz indicate that the samples have been completely cleansed of all organic matter. Phenomenon's aromatic rings C-C bond and its C-O link bend in the 1381 cm^{-1} band, respectively. As the C-O bond stretches asymmetrically in polymeric material, it creates a band at 1120 cm^{-1}.

3.4. SEM and TEM Analyses. The morphology of TiO_2 nanoparticles was studied using SEM. Before reduction, the crystalline size is 29 nm. Figure 7(a) shows the average particle diameter of the TiO_2 particles synthesized in this method to be 27 nm. Powder particles were found to be clumped together. EDAX analysis was used to determine the composition of the TiO_2 nanoparticles. In Figure 7(b), the only metals with peak values were titanium (Ti) and oxygen (O); no other metals' peak values were presented. Thus, the existence of TiO_2 particles has been confirmed.

Photocatalytic dye degradation is dependent on nanoparticles' surface shape and size. The obtained TiO_2 nanoparticles sizes were found to be 27 nm, and their shape is spherical shape with some irregular shapes (Figure 7(c)). The irregular shapes and adjunct nanoparticles were formed from the plant nutrients. The obtained shapes and sizes were well coincided with XRD and SEM results. The excess amount of plant nutrients and surface plant molecules was reensured from FTIR and EDX analyses.

3.5. Photocatalytic Activity. TiO_2 nanoparticles degrades methylene blue (MB) solution, as seen in Figures 8(a)–8(c). The initial concentration of MB dye is 10 ppm. TiO_2 without sunlight light degrades methylene blue resolution much slower than TiO_2 with sunlight light. Figure 6 depicts the photocatalytic activity of TiO_2 using sunlight irradiations [41].

In the absence of ultraviolet light, there will be no photocatalytic reaction. The MB breakdown of around 9 percent is not due to a photocatalytic process, but rather to MB adsorption by TiO_2 particles in the presence of oxygen. The approach that makes use of visual destruction rays, on the other hand, has produced considerable outcomes in research. The degradation of MB to 94 percent by TiO_2 nanoparticles may take place in as little as two hours. According to this finding, photocatalytic activity occurs only when light (visible light) is present, and this may be explained by the photocatalytic process in action.

The photocatalytic mechanism of TiO_2 can be explained from

$$\begin{aligned}
TiO_2 + h\vartheta &\longrightarrow e^-_{cb} + h^+_{\vartheta b}\\
h^+_{\vartheta b} + H_2O &\longrightarrow H^+ + HO^*\\
e^-_{cb} + O_2 &\longrightarrow O_2^{-*}\\
O_2^{-*} + H^+ &\longrightarrow HO_2^*\\
HO_2^* + HO_2^* &\longrightarrow H_2O_2 + O_2\\
H_2O_2 + e^-_{cb} &\longrightarrow HO^* + HO^-\\
H_2O_2 + h\vartheta &\longrightarrow 2HO^*\\
R + HO^* &\longrightarrow CO_2 + H_2O
\end{aligned} \tag{4}$$

As shown in Figure 8, the photocatalytic mechanism of TiO_2 can be described. When TiO_2 NPs absorb incident sunlight irradiation (i.e., $hv > E_g$), electron (e^-) and hole (h^+) pairs are created in the TiO_2 NPs. Photogenerated electrons and holes wander through the material, eventually reaching the surface of TiO_2 NPs. The electrons will react with the oxygen to form superoxide radicals, while the holes will react with the water to form hydroxyl radicals (OH·) [42, 43]. Both of these free radicals will react with nearby water-soluble molecules, particularly organic compounds. The organic molecule (MB) will be decomposed by the hydroxyl radical into water (H_2O) and carbon dioxide (CO_2). The

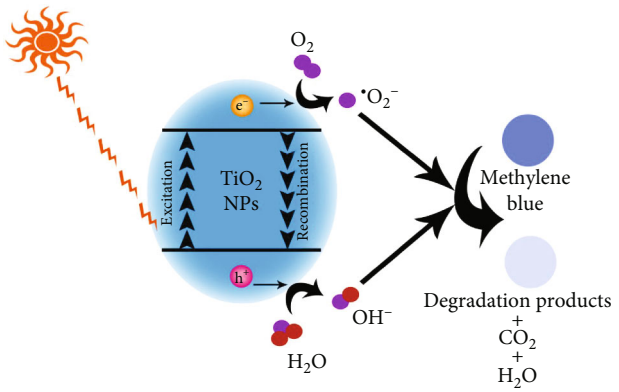

FIGURE 9: Photocatalysis mechanism for TiO_2 nanoparticles under UV light illumination to degrade MB dye [41].

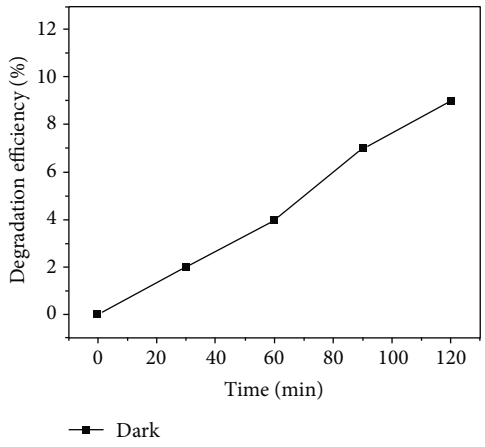

FIGURE 10: Photocatalysis mechanism for TiO_2 nanoparticles in the absence of UV light illumination to degrade MB dye.

superoxide radicals ($O_2^{\cdot -}$) react with water (H_2O) to form hydrogen peroxide (H_2O_2), when they react with electrons to produce hydroxyl radicals. Finally, peroxide reacts with light energy (hυ) to produce another hydroxyl radical (OH·). The MB will be decomposed by this hydroxyl radical (OH·) into water (H_2O) and carbon dioxide (CO_2).

The photocatalytic activities of TiO_2 nanoparticles were also examined in various settings (with visible light) and pH conditions for acidic (pH = 2), neutral (pH = 7), and base (pH = 12). Figure 9 depicts the findings of the photocatalytic experiment. The reaction produces the hydroxyl radical (OH·) in the neutral state as shown in

$$h_{vb}^{+} + H_2O \longrightarrow H^{+} + HO^{*} \quad (5)$$

In Figure 10, the photocatalytic mechanism of TiO_2 can be described in the absence of UV light.

The hydroxyl radical can also be created directly under alkaline conditions from the (OH) ion, which interacts with the hole in the following reaction as shown in

$$\begin{aligned} h_{vb}^{+} + OH^{-} &\longrightarrow HO^{*} \\ H^{+} + e^{-} &\longrightarrow H^{*} \\ H^{*} + HO^{*} &\longrightarrow H_2O \end{aligned} \quad (6)$$

As a result, the hydroxyl radical (OH·) will be more abundant under alkaline conditions, improving its photocatalytic ability. Acidic conditions are in excess, and this surplus will interact with free electrons (e^-) to form radicals (OH·). There will be a backlash and a return to when this radical (OH·) emerges. As a result, the hydroxyl radical (OH·) produced in alkaline conditions will be more abundant, improving its photocatalytic capacity. There is an excess of (H^+) under acidic circumstances, and this surplus (H^+) interacts with free electrons (e^-) to create radicals (H^+). The creation of this radical (H^+) will result in a reaction with (OH), and (H^+) will revert to H_2O.

Figure 1(a) shows the degradation efficacy of biosynthesized TiO_2 NPs with various pH, Figure 1(b) shows the C/C_0 absorption rate, and Figure 1(c) shows the photocatalytic degradation kinetics study of the biosynthesized TiO_2 NPs with various pH. This reduces the quantity of hydroxyl radical produced, resulting in a decrease in photocatalytic activity under acidic circumstances. It implies that photocatalytic activity is better in alkaline pH settings than in neutral pH situations and that photocatalytic activity is slower in acid pH conditions than in neutral pH conditions.

4. Conclusion

(1) Using only a few easy processes, this study proved how to produce TiO_2 nanoparticles from Aloe vera plant extract in an environmentally and economically friendly manner. The tetragonal structure of the synthesized NPs was confirmed using XRD analysis

(2) It was determined that the nanoparticles have a diameter of 27 nm by applying the Debye-Scherrer equation

(3) To confirm the dimensions and structural characteristics of the nanoparticles, SEM and TEM are used. According to the findings of the UV-vis tests, TiO_2 nanoparticles were created, with a high peak at 298 nm

(4) Calculated using the Tauc plot, the nanoparticle bandgap was estimated at 3.48 eV

(5) To put it another way, the MB dye degraded by 94% when exposed to UV light. Wastewater treatment and environmental remediation operations rely on the ecologically benign production of TiO_2 nanoparticles

Data Availability

The data used to support the findings of this study are included in the article.

Conflicts of Interest

The authors declare that they have no conflicts of interest regarding the publication of this paper.

References

[1] A. Nanda and M. Saravanan, "Biosynthesis of silver nanoparticles from Staphylococcus aureus and its antimicrobial activity against MRSA and MRSE," *Nanomedicine*, vol. 5, no. 4, pp. 452–456, 2009.

[2] T. Ochiai and A. Fujishima, "Photoelectrochemical properties of TiO_2 photocatalyst and its applications for environmental purification," *Journal of Photochemistry and Photobiology C: Photochemistry Reviews*, vol. 13, no. 4, pp. 247–262, 2012.

[3] Z. Xing, J. Zhang, J. Cui et al., "Recent advances in floating TiO_2-based photocatalysts for environmental application," *Applied Catalysis, B: Environmental*, vol. 225, pp. 452–467, 2018.

[4] S. MiarAlipour, D. Friedmann, J. Scott, and R. Amal, "TiO_2/porous adsorbents: recent advances and novel applications," *Journal of Hazardous Materials*, vol. 5, no. 341, pp. 404–423, 2018.

[5] S. Marimuthu, A. AbdulRahuman, C. Jayaseelan et al., "Acaricidal activity of synthesized titanium dioxide nanoparticles using Calotropis gigantea against Rhipicephalus microplus and Haemaphysalisbispinosa," *Asian Pacific Journal of Tropical Medicine*, vol. 6, no. 9, 2013.

[6] S. Banhart, E. M. Saied, A. Martini et al., "Improved plaque assay identifies a novel anti-chlamydia ceramide derivative with altered intracellular localization," *Antimicrobial Agents and Chemotherapy*, vol. 58, no. 9, pp. 5537–5546, 2014.

[7] E. F. El-Belely, M. Farag, H. A. Said et al., "Green synthesis of zinc oxide nanoparticles (ZnO-NPs) using Arthrospira platensis (class: Cyanophyceae) and evaluation of their biomedical activities," *Nanomaterials*, vol. 11, no. 1, p. 95, 2021.

[8] M. Soliman, H. A. Alhaithloul, K. R. Hakeem, B. M. Alharbi, M. El-Esawi, and A. Elkelish, "Exogenous nitric oxide mitigates nickel-induced oxidative damage in eggplant by upregulating antioxidants, osmolyte metabolism, and glyoxalase systems," *Plants*, vol. 8, no. 12, p. 562, 2019.

[9] H. S. A. Al-Shmgani, W. H. Mohammed, G. M. Sulaiman, and A. H. Saadoon, "Biosynthesis of silver nanoparticles from Catharanthus roseus leaf extract and assessing their antioxidant, antimicrobial, and wound-healing activities," *Artificial Cells, Nanomedicine, and Biotechnology*, vol. 45, no. 6, pp. 1234–1240, 2017.

[10] M. Shah, D. Fawcett, S. Sharma, S. K. Tripathy, and G. E. J. Poinern, "Green synthesis of metallic nanoparticles via biological entities," *Gérrard Eddy Jai Poiner Materials*, vol. 8, no. 11, pp. 7278–7308, 2015.

[11] S.-J. Bao, C. Lei, M. W. Xu, C. J. Cai, and D. Z. Jia, "Environment-friendly biomimetic synthesis of TiO_2 nanomaterials for photocatalytic application," *Nanotechnology*, vol. 23, no. 20, article 205601, 2012.

[12] S. B. NurhidayatullailiMuhdJulkapli and S. B. A. Hamid, "Recent advances in heterogeneous photocatalytic decolorization of synthetic dyes," *The Scientific WorldJournal*, vol. 2014, article 692307, 25 pages, 2014.

[13] S. Shanavas, A. Priyadharsan, S. Karthikeyan et al., "Green synthesis of titanium dioxide nanoparticles using Phyllanthus niruri leaf extract and study on its structural, optical and morphological properties," *Materials Today: Proceedings*, vol. 26, pp. 3531–3534, 2020.

[14] M. M. Viana, V. F. Soares, and N. D. S. Mohallem, "Synthesis and characterization of TiO_2 nanoparticles," *Ceramics International*, vol. 36, no. 7, 2010.

[15] N. V. DejanVerhovsek, M. K. UrskaLavrencicStangar, K. Zagar, and M. Ceh, "The synthesis of anatase nanoparticles and the preparation of photocatalytically active coatings based on wet chemical methods for self-cleaning applications," *International Journal of Photoenergy*, vol. 2012, Article ID 329796, 10 pages, 2012.

[16] M. I. Dar, A. K. Chandiran, M. Graetzel, M. Nazeeruddin, and S. Shivashankar, "Controlled synthesis of TiO_2 nanoparticles and nanospheres using a microwave assisted approach for their application in dye-sensitized solar cells," *Journal of Materials Chemistry A*, vol. 2, no. 6, pp. 1662–1667, 2014.

[17] J. M. Abisharani, S. Devikala, R. Dinesh Kumar, M. Arthanareeswari, and P. Kamaraj, "Green synthesis of TiO_2 nanoparticles using Cucurbita pepo seeds extract," *Materials Today: Proceedings*, vol. 14, pp. 302–307, 2019.

[18] B. Joseph and S. J. Raj, "Pharmacognostic and phytochemical properties of Aloe vera Linn –an overview," *International Journal of Pharmaceutical Sciences Review and Research*, vol. 4, no. 2, pp. 106–110, 2010.

[19] R. Wynn, "Aloe vera Gel: Update for dentistry," *General Dentistry*, vol. 53, no. 1, pp. 6–9, 2005.

[20] A. Bozzi, C. Perrin, S. Austin, and V. F. Arce, "Quality and authenticity of commercial aloe vera gel powders," *Food Chemistry*, vol. 103, no. 1, pp. 22–30, 2007.

[21] U. Nandal and R. L. Bhardwaj, "Aloe vera: a valuable wonder plant for food, medicine and cosmetic use - a review," *International Journal of Pharmaceutical Sciences Review and Research*, vol. 13, no. 1, pp. 59–67, 2012.

[22] S. Kumar, A. Yadav, M. Yadav, and J. P. Yadav, "Effect of climate change on phytochemical diversity, total phenolic content and in vitro antioxidant activity of Aloe vera (L.) Burm.f," *BMC Research Notes*, vol. 10, no. 1, p. 60, 2017.

[23] P. Dey, S. Dutta, A. Chowdhury, A. P. Das, and T. K. Chaudhuri, "Variation in phytochemical composition reveals distinct divergence of Aloe vera (L.) Burm.f. from other Aloe species: rationale behind selective preference of Aloe vera in nutritional and therapeutic Use," *Journal of Evidence-Based Complementary & Alternative Medicine*, vol. 22, no. 4, pp. 624–631, 2017.

[24] R. Bista, A. Ghimire, and S. Subedi, "Phytochemicals and antioxidant activities of Aloe vera (Aloe barbadensis)," *Journal of Nutritional Science and Healthy Diet*, vol. 1, no. 1, pp. 25–36, 2020.

[25] J. Rajkumari, C. Maria Magdalane, B. Siddhardha et al., "Synthesis of titanium oxide nanoparticles using Aloe barbadensis mill and evaluation of its antibiofilm potential against Pseudomonas aeruginosa PAO1," *Journal of Photochemistry and Photobiology B: Biology*, vol. 201, article 111667, 2019.

[26] J. Jeevanandam, Y. S. Chan, and Y. J. W. Y. S. Hii, "Biogenic Synthesis of magnesium oxide nanoparticles using Aloe barbadensis leaf latex extract," in *IOP Conference Series: Materials Science and Engineering, Volume 943, 2nd International Conference on Materials Technology and Energy*, Miri, Sarawak, Malaysia, 2020.

[27] N. I. Rasli, H. Basri, and Z. Harun, "Zinc oxide from aloe vera extract: two-level factorial screening of biosynthesis parameters," *Heliyon*, vol. 6, no. 1, article e03156, 2020.

[28] Y. Fang, X. Y. Yu, and X. W. Lou, "Nanostructured electrode materials for advanced sodium-ion batteries," *Matter*, vol. 1, no. 1, 2019.

[29] M. Taghdiri, "Selective Adsorption and Photocatalytic Degradation of Dyes Using Polyoxometalate Hybrid Supported on Magnetic Activated Carbon Nanoparticles under Sunlight, Visible, and UV Irradiation," *International Journal of Photoenergy*, vol. 2017, Article ID 8575096, 15 pages, 2017.

[30] R. Rajendhiran, V. Deivasigamani, J. Palanisamy, S. Masan, and S. Pitchaiya, "Terminalia catappa and carissa carandas assisted synthesis of Tio_2 nanoparticles - a green synthesis approach," *The Netherlands*, vol. 45, pp. 2232–2238, 2021.

[31] M. Lal, P. Sharma, and C. Ram, "Calcination temperature effect on titanium oxide (TiO_2) nanoparticles synthesis," *Optik*, vol. 241, article 166934, 2021.

[32] M. K. Debanath, S. Karmakar, and J. P. Borah, "Structural characterization of ZnO nanoparticles synthesized by wet chemical method," *Advanced Science, Engineering and Medicine*, vol. 4, no. 4, pp. 306–311, 2012.

[33] L. Zhang, Q. Zhang, H. Xie et al., "Electrospun titania nanofibers segregated by graphene oxide for improved visible light photocatalysis," *Applied Catalysis B: Environmental*, vol. 201, pp. 470–478, 2017.

[34] L. Zhang, P. Ma, L. Dai, S. Li, W. Yu, and J. Guan, "In situ crystallization and growth of TiO 2 nanospheres between MXene layers for improved adsorption and visible light photocatalysis," *Catalysis Science & Technology*, vol. 11, no. 11, pp. 3834–3844, 2021.

[35] L. Zhang, L. Dai, X. Li, W. Yu, S. Li, and J. Guan, "3D structured TiO 2-based aerogel photocatalyst for the high-efficiency degradation of toluene gas," *New Journal of Chemistry*, vol. 46, no. 5, pp. 2272–2281, 2022.

[36] "Large scaled synthesis of heterostructured electrospun TiO_2/SnO_2 nanofibers with an enhanced photocatalytic activity," *Journal of the Electrochemical Society*, vol. 164, no. 9, pp. H651–H656, 2017.

[37] V. Balakumar and S. Selvaraj, "AmanullaBaishnisha, Sellamuthu Kathiresan, in-situ growth of TiO_2@B-doped g-C_3N_4 core-shell nanospheres for boosts the photocatalytic detoxification of emerging pollutants with mechanistic insight," *Applied Surface Science*, vol. 577, article 151924, 2022.

[38] K. Lingaraju, R. B. Basavaraj, K. Jayanna et al., "Biocompatible fabrication of TiO_2 nanoparticles: antimicrobial, anticoagulant, antiplatelet, direct hemolytic and cytotoxicity properties," *Inorganic Chemistry Communications*, vol. 127, p. 108505, 2021.

[39] A. L. Stanford and J. M. Tanner, *Physics for Students of Science and Engineering*, Academic Press, 1985.

[40] Y. M. Hunge, A. Uchida, Y. Tominaga et al., "Visible light-assisted photocatalysis using spherical-shaped $BiVO_4$ photocatalyst," *Catalysts*, vol. 11, no. 4, p. 460, 2021.

[41] K. Huszla, M. Wysokowski, A. Zgoła-Grześkowiak et al., "UV-light photocatalytic degradation of non-ionic surfactants using ZnO nanoparticles," *International journal of Environmental Science and Technology*, vol. 19, no. 1, pp. 173–188, 2022.

[42] S. Umamaheswari Rajaji, E. G. D. Rani, S.-M. Chen et al., "Synergistic photocatalytic activity of SnO_2/PANI nanocomposite for the removal of direct blue 15 under UV light irradiation," *Ceramics International*, vol. 47, no. 20, 2021.

[43] E. Moretti, E. Cattaruzza, C. Flora, A. Talon, E. Casini, and A. Vomiero, "Photocatalytic performance of Cu-doped titania thin films under UV light irradiation," *Applied Surface Science*, vol. 553, article 149535, 2021.